Journal of Biomedical Optics

SPIEDigitalLibrary.org/jbo

Speckle reduction in optical coherence tomography imaging by affine-motion image registration

David Alonso-Caneiro
Scott A. Read
Michael J. Collins

SPIE

Speckle reduction in optical coherence tomography imaging by affine-motion image registration

David Alonso-Caneiro, Scott A. Read, and Michael J. Collins
Queensland University of Technology, Contact Lens and Visual Optics Laboratory, School of Optometry, Brisbane, QLD 4059 Australia

Abstract. Signal-degrading speckle is one factor that can reduce the quality of optical coherence tomography images. We demonstrate the use of a hierarchical model-based motion estimation processing scheme based on an affine-motion model to reduce speckle in optical coherence tomography imaging, by image registration and the averaging of multiple B-scans. The proposed technique is evaluated against other methods available in the literature. The results from a set of retinal images show the benefit of the proposed technique, which provides an improvement in signal-to-noise ratio of the square root of the number of averaged images, leading to clearer visual information in the averaged image. The benefits of the proposed technique are also explored in the case of ocular anterior segment imaging. [DOI: 10.1117/1.3652713]

Keywords: speckle reduction; optical coherence tomography; image registration.

Paper 11402LR received Jul. 26, 2011; revised manuscript received Sep. 8, 2011; accepted for publication Sep. 27, 2011; published online Nov. 17, 2011.

1 Introduction

Due to its noninvasive nature, high resolution, and imaging depth capabilities, optical coherence tomography (OCT) has become a commonly used biomedical imaging technique, especially in the field of ophthalmology.[1,2] OCT imaging of the retina and anterior eye is now widely used in ophthalmic clinical and research practice. Unfortunately, the technique is sensitive to speckle (i.e., signal-degrading speckle),[3] which limits the amount of information and the signal-to-noise ratio (SNR) of the image, causing difficulties for image interpretation. This can potentially complicate the clinical diagnosis and reduces the accuracy of the segmentation of the anatomical layers of the tissues in the OCT images. Therefore it is desirable to suppress the speckle in the images.

In the field of OCT, a number of approaches have been proposed to reduce speckle. Among them, the two most widely used approaches involve either hardware- or software-based techniques. The hardware-based techniques rely on the uncorrelated speckle between different angles, positions, or wavelengths, such as the angular[4,5] and frequency[6] compounding techniques. Another recent hardware-based approach to speckle reduction is the technique of strain compounding,[7,8] which compresses the sample to create the uncorrelated speckle. However, all of these hardware-based techniques cannot be easily adapted to standard commercial OCT units. On the other hand, the software-based techniques[9–11] correspond to a set of post-processing algorithms used to reduce the speckle after the measurement is taken and the image is formed. These techniques may therefore be applied to improve the image quality from current OCT ophthalmic instruments.

The software-based techniques can be subdivided as methods involving single B-scan image filtering or multiple uncorrelated B-scan averaging. The former method uses a smoothing filter function to reduce the speckle in a single image, such as the adaptive Wiener filter[11] and adaptive complex diffusion (ACD)[9] or more sophisticated volumetric approaches [i.e., curvelet transform[12]], while the latter uses the average of multiple consecutive uncorrelated B-scans. If the speckle is uncorrelated between the multiple B-scans, the SNR of the resulting averaged image should increase by a factor of $\sqrt{N}$, where N indicates the number of averaged B-scans.[3] In ophthalmic imaging, the natural small eye movements help to produce an uncorrelated set of B-scans. The main challenge with this technique is the registration of the images to account for the effect of eye movements between multiple B-scans. Jorgensen et al.[10] proposed one of the earlier techniques to align OCT images based on dynamic programming to align consecutive images in the vertical and horizontal directions (i.e., translation motion). Given that the eye is capable of more complex movements (e.g., rotation, torsion), techniques of image registration that account for higher degrees of eye movement may result in improved performance.

To date only a small fraction of the available commercial OCT instruments are able to perform real-time eye tracking. The Spectralis (Heidelberg Engineering, Heidelberg, Germany) and Spectral OCT/SLO (OPKO/OTI, Miami, Florida) combine a scanning laser ophthalmoscope with OCT to produce tracking laser tomographs. This enables highly precise alignment of OCT images, making the registration of consecutive B-scans simple. For the other commercially available OCT systems, software-based tools are required for image registration. However, only a few of these systems (3D OCT-2000, Topcon, Japan and Cirrus HD-OCT, Carl Zeiss, Germany) currently provide these tools.

In this paper an alternative technique of image registration, based on hierarchical model-based motion (HMBM), is presented and applied to OCT images for the first time. The technique uses an affine-motion model to register images, which

Address all correspondence to: David Alonso-Caneiro, Queensland University of Technology, School of Optometry, Victoria Park Rd, Kelvin Grove Brisbane, QLD 4059 Australia; Tel: 0061731385716; E-mail: d.alonsocaneiro@qut.edu.au.

1083-3668/2011/16(11)/116027/5/$25.00 © 2011 SPIE

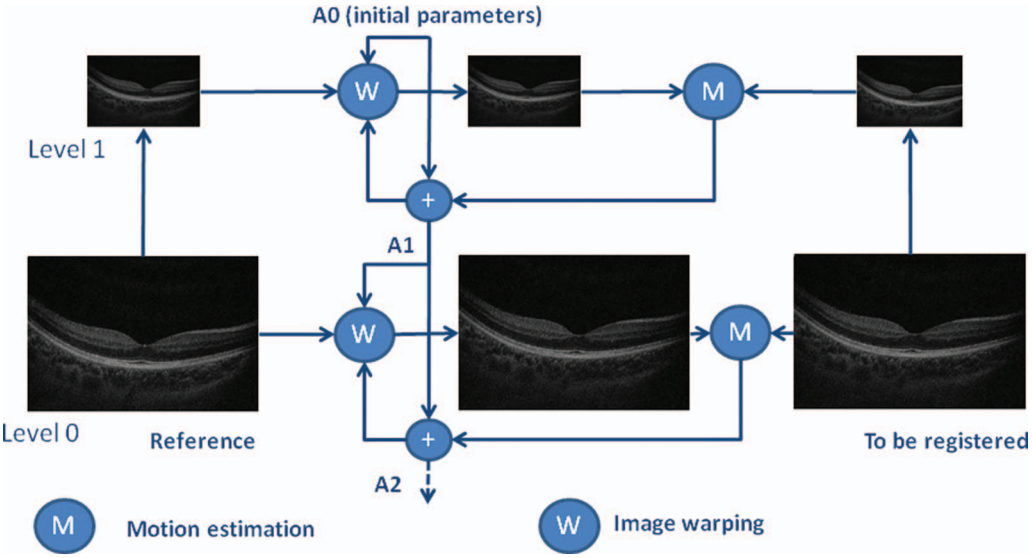

Fig. 1 A two-level schematic of the HMBM. After the images are rescaled (pyramid), the algorithm is executed from top to bottom, where the motion parameters (A0 to A2) are transferred to the next level.

has proven to be suitable for local deformations[7,8] and involves the following image transformations: translation, scaling, rotation, and shear.[13] While the proposed technique can produce a loss of spatial resolution, the result when applied to a set of OCT B-scan images shows the potential of the technique to enhance the standard instrument functionality. We investigate the results of this technique in imaging of the posterior and anterior segment of the human eye.

2 Methods

The HMBM estimation proposed by Bergen at al.[14] provides a framework for the alignment of images. Figure 1 shows the schematic of a two-level alignment procedure, which can be divided into four major components: pyramid construction, motion estimation, image warping, and coarse-to-fine refinement. Basically, the reference and the image to be registered are reshaped into a smaller resolution image, based on the Laplacian Pyramid.[13] The Laplacian Pyramid decomposes the original image into a hierarchy of images such that each level corresponds to a different band of image frequencies. Starting from the lower resolution image, the motion estimation algorithm is processed, which estimates the motion based on a constrained model (i.e., affine model). The affine transformation/warping follows,

$$u(x, y) = a_1 + a_2 x + a_3 y,$$
$$v(x, y) = a_4 + a_5 x + a_6 y,$$

where (x, y) represents the coordinates on the original image and (u, v) on the warped image. Once the estimates of the motion parameter (i.e., $a_1 ... a_6$) are obtained in Level 1 of the procedure, they are then transferred to the next level of the pyramid, following the coarse-to-fine scheme and the procedure continues until reaching the lowest level.

In our scheme, a four-level HMBM was implemented. The first image of the set is used as a reference, to which the rest of the images are subsequently registered. Once the alignment is completed, the average of all B-scans is taken as the final image. The HMBM framework provides two major benefits, the computation of large displacement can be done using low resolution images and is therefore computationally efficient, but more importantly the method is robust.[14]

To assess the benefit of the technique based on the affine registration, the proposed method is benchmarked against a rigid-registration based entirely on translation, which was implemented using FFT-based techniques.[15] This motion-model has been used in previous publications involving OCT B-scan registration.[10] Additionally, we also performed a comparison with the other software-based method of speckle reduction, single B-scan image filtering techniques. A large body of literature regarding image filtering is available, and in this work we have selected the adaptive Wiener filter[11] and the ACD[9] as two representative examples.

3 Results and Discussion

A retrospective data set of retinal OCT scans from 20 subjects, in which each subject had one set of 50 consecutive horizontal, 5 mm foveal raster B-scans taken (B-scan = 1500 A-scans) was used to assess the technique.[16] The Copernicus SD OCT HR (Optopol Technology S.A., Zawiercie, Poland) instrument was used to collect the OCT data. The system uses a superluminescent diode of 850 nm and allows the capture of 52,000 A-scans/s, with a 3 μm axial and a 5 μm transversal resolution in tissue. The A-scan contains 855 pixels. Similar to other commercial units, it does not track eye movements, however it is able to capture multiple and consecutive retinal B-scans using its so-called animation measurement mode. The proposed HMBM image processing techniques were used to align and register the 50 B-scans for each subject. Figure 2 shows an example of a single B-scan [Fig. 2(a)] and the aligned average B-scan of a representative subject [Fig. 2(b)]. A zoomed region was added in the left side of the images to illustrate the speckle reduction and any potential loss of spatial resolution.

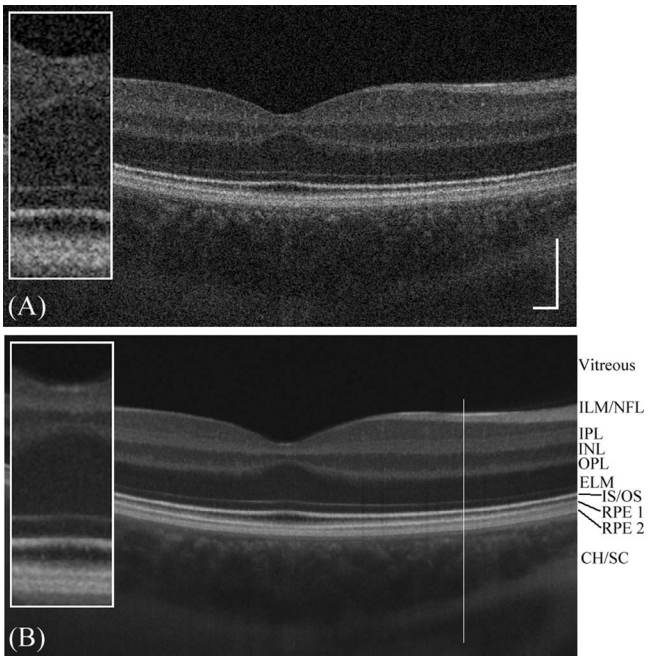

Fig. 2 B-scan images of the central foveal region of the human retina. (a) Single B-scan and (b) B-scan after HMBM speckle reduction. Note the enhanced definition of the retinal features in the speckle reduced image. ILM/NFL, inner limiting membrane/nerve fiber layer; IPL, inner plexiform layer; INL, inner nuclear layer; OPL, outer plexiform layer; ELM, external limiting membrane; IS/OS junction between the inner and outer segment of the photoreceptors; RPE, retinal pigment epithelium; CH/SC junction between the choroid and sclera. Insets show a zoomed region from the central portion of the images. The scale bars represent 200 μm.

Two image quality metrics, SNR and contrast-to-noise ratio (CNR) were used to assess the performance of the technique. The SNR is defined as SNR $= \mu_b/\sigma_b$, where μ_b and σ_b are the mean and the standard deviation of the intensity, which is calculated in the background region of the image (for the retinal image it is the vitreous-humor area).[4] The CNR is calculated as follows:

$$\mathrm{CNR} = (1/R)\sum_{r=1}^{R}\left(\mu_r - \mu_b/\sqrt{\sigma_r^2 + \sigma_b^2}\right),$$

where μ_r and σ_r are the mean and the standard deviation, respectively, of the intensity from a set of six different regions of interest that were manually selected in the image.[11]

For the 20 different scans, we estimated the average SNR and CNR improvement based on the number of averaged images and present these data in Fig. 3. Both metrics increase (improve) as the number of averaged images increases. For the HMBM technique, the improvement in SNR obtained is close to the square root of the number of averaged images; this improvement is due to the reduction of the standard deviation of the noise. In both image quality metrics (SNR and CNR) the affine-motion model performs better than the rigid translation model (TM). For the single filter (ACF and Wiener), the results are comparable to the average of 14 B-scans for the SNR and around 5 B-scans for the CNR.

The reduction in speckle with the registration technique is also evident when looking at a single A-scan with different techniques. Figure 4 presents a single A-scan profile taken from Fig. 2(b) (vertical white solid line), with the retinal layer information provided in the profile in Fig. 2(b). Following the HMBM registration technique, the reduction in noise appears to enhance the layer/edge separation (Fig. 4). Although the peak intensity in the averaged image is slightly lower than in the single B-scan at some locations, the reduction in surrounding noise allows the features in the image to be more clearly delineated (Fig. 4). We have also presented a zoomed region of the IS/OS boundary (Fig. 4 inset), comparing the profile of the different techniques versus a single B-scan profile. Taking the full width at

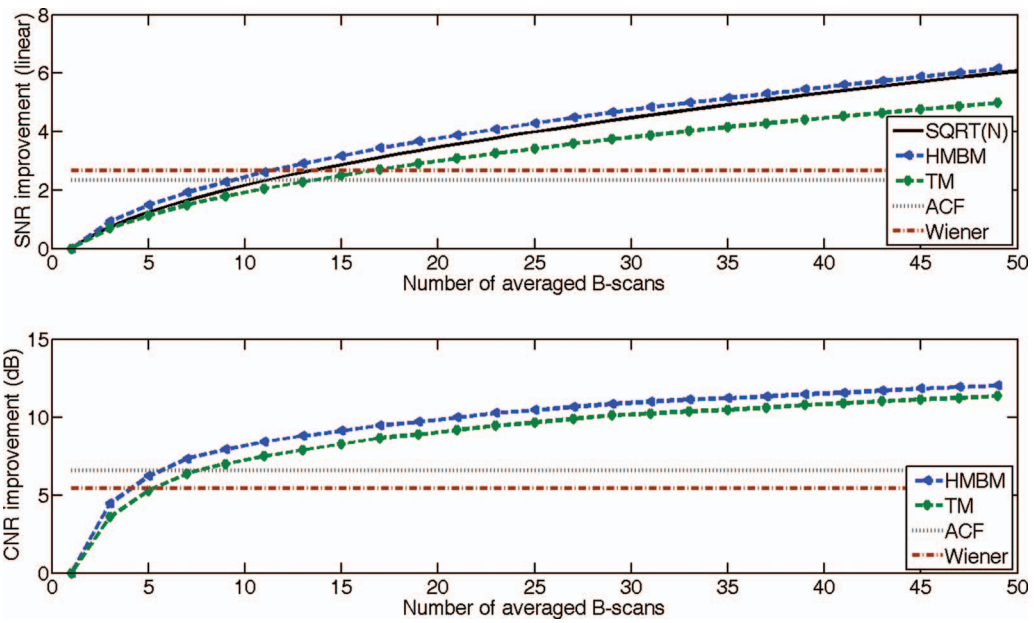

Fig. 3 Average SNR and CNR improvement compared to a single B-scan, as a function of the number of averaged B-scans (HMBM-Hierarchical Model-Based Motion, TM- translation model). The horizontal lines represent the performance of the single B-scan filter (ACD-adaptive complex diffusion, Wiener).

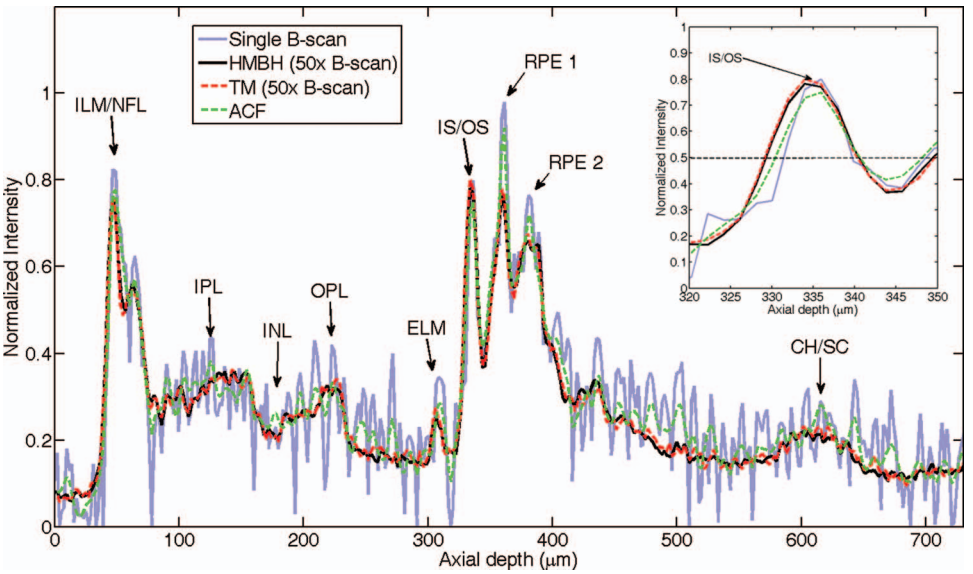

Fig. 4 Example of a single A-scan profile of the foveal retinal image from Fig. 2(b) (vertical white solid line). Inset shows a zoomed region around the IS/OS boundary.

half maximum, we estimated that the profile broadens by about 2.5 μm for the $\times 50$ averages images. Thus, some loss of spatial resolution is observed in the proposed technique, although this value is below the actual resolution of the system (i.e., 3 μm).

Overall, while there is some slight loss of spatial resolution and the peak intensity in the averaged image is slightly lower than the single B-scan at some locations, the overall reduction in surrounding noise allows the features in the image to be more clearly delineated (Fig. 4). The SNR and CNR improvement for the single B-scan following filtering using TM and ACF procedures does not appear to highlight all the layers as effectively as the HMBM registration technique.

Apart from the benefit in terms of speckle reduction, another major benefit of the registration is the improvement in the image quality and enhancement of features that could be masked in a single B-scan due to the image speckle. An example of this for imaging the anterior eye is shown in Fig. 5, which corresponds to a set of B-scans of the cornea while wearing a contact lens (purposely fit steep). An SNR improvement of 6 dB is obtained with the proposed technique. It is worth noting that after registration the epithelium and Bowman's membrane are more clearly defined.

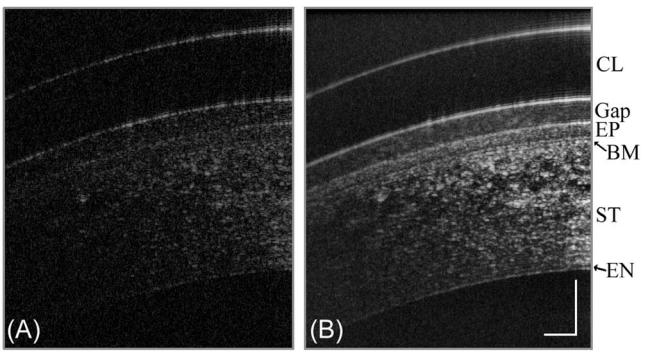

Fig. 5 B-scan of a human cornea with a contact lens. (a) Single B-scan and (b) B-scan after HMBM speckle reduction. CL, contact lens; Gap, gap between contact lens-cornea EP, epithelium; BM, Bowman's membrane, ST, stroma; EN, endothelium. The scale bars represent 200 μm.

4 Conclusions

We demonstrate the efficacy of a hierarchical model-based motion technique to reduce speckle in OCT images. The application of this method to the post-processing of OCT images leads to substantial improvements in image quality, which could greatly benefit the identification of clinical features and diagnostic ability of OCT imaging. An SNR improvement of $\sqrt{N}$ was shown for the technique. Although the proposed technique can be affected by the loss in spatial resolution, any loss associated with this technique is minor compared to the high SNR improvement which reveals image details that were previously obscured by the signal reducing speckle in the single B-scan (e.g., CH/SC junction in Figs. 2 and 4). As with other biomedical imaging techniques, the affine model estimation seems to be suitable for registration of consecutive OCT B-scans and to produce an averaged image with reduced speckle.

References

1. W. Drexler, U. Morgner, R. K. Ghanta, F. X. Kärtner, J. S. Schuman, and J. G. Fujimoto, "Ultrahigh-resolution ophthalmic optical coherence tomography," *Nat. Med.* **7**(4), 502–507 (2001).
2. M. Wojtkowski, R. Leitgeb, A. Kowalczyk, T. Bajraszewski, and A. F. Fercher, "*In vivo* human retinal imaging by Fourier domain optical coherence tomography," *J. Biomed. Opt.* **7**(3), 457–463 (2002).
3. J. M. Schmitt, S. H. Xiang, and K. M. Yung, "Speckle in optical coherence tomography," *J. Biomed. Opt.* **4**(1), 95–105 (1999).
4. Y. Watanabe, H. Hasegawa, and S. Maeno, "Angular high-speed massively parallel detection spectral-domain optical coherence tomography for speckle reduction," *J. Biomed. Opt.* **16**(6), 060504 (2011).
5. N. Iftimia, B. E. Bouma, and G. J. Tearney, "Speckle reduction in optical coherence tomography by "path length encoded" angular compounding," *J. Biomed. Opt.* **8**(2), 260–263 (2003).
6. M. Pircher, E. Götzinger, R. Leitgeb, A. F. Fercher, and C. K. Hitzenberger, "Speckle reduction in optical coherence tomography by frequency compounding," *J. Biomed. Opt.* **8**(3), 030512 (2003).

7. B. F. Kennedy, T. R. Hillman, A. Curatolo, and D. D. Sampson, "Speckle reduction in optical coherence tomography by strain compounding," *Opt. Lett.* **35**(14), 2445–2447 (2010).
8. B. F. Kennedy, A. Curatolo, T. R. Hillman, C. M. Saunders, and D. D. Sampson, "Speckle reduction in optical coherence tomography images using tissue viscoelasticity," *J. Biomed. Opt.* **16**(2), 0506 (2011).
9. R. Bernardes, C. Maduro, P. Serranho, A. Araújo, S. Barbeiro, and J. Cunha-Vaz, "Improved adaptive complex diffusion despeckling filter," *Opt. Express* **18**(23), 24048–24059 (2010).
10. T. M. Jørgensen, J. Thomadsen, U. Christensen, W. Soliman, and B. Sander, "Enhancing the signal-to-noise ratio in ophthalmic optical coherence tomography by image registration—method and clinical examples," *J. Biomed. Opt.* **12**(4), 041208 (2007).
11. A. Ozcan, A. Bilenca, A. E. Desjardins, B. E. Bouma, and G. J. Tearney, "Speckle reduction in optical coherence tomography images using digital filtering," *J. Opt. Soc. Am. A* **24**(7), 1901–1910 (2007).
12. Z. Jian, L. Yu, B. Rao, B. J. Tromberg, and Z. Chen, "Three-dimensional speckle suppression in optical coherence tomography based on the curvelet transform," *Opt. Express* **18**(2), 1024–1032 (2010).
13. R. C. Gonzalez and R. E. Woods, *Digital Image Processing*, Pearson Prentice Hall, NJ (2002).
14. J. Bergen, P. Anandan, K. Hanna, and R. Hingorani, *Hierarchical Model-Based Motion Estimation*, pp. 237–252, Springer, New York (1992).
15. B. S. Reddy and B. N. Chatterji, "An FFT-based technique for translation, rotation, and scale-invariant image registration," *IEEE Trans. Image Process.* **5**(8), 1266–1271 (1996).
16. S. A. Read, M. J. Collins, and D. Alonso-Caneiro, "Validation of optical low coherence reflectometry retinal and choroidal biometry," *Optom. Vision Sci.* **88**(7), 855–863 (2011).